JIPB Journal of Integrative Plant Biology

Research Article
https://doi.org/10.1111/jipb.13889

The LUX–SWI3C module regulates photoperiod sensitivity in *Arabidopsis thaliana*

Jianhao Wang[1,2†], Huan Liu[1†], Hong Li[1†], Fan Wang[1†], Songguang Yang[2], Lin Yue[1], Shuangrong Liu[1], Baohui Liu[1], Mingkun Huang[3*], Fanjiang Kong[1*] and Zhihui Sun[1*]

1. Guangdong Key Laboratory of Plant Adaptation and Molecular Design, Guangzhou Key Laboratory of Crop Gene Editing, Innovative Center of Molecular Genetic and Evolution, School of Life Science, Guangzhou University, Guangzhou 510006, China
2. Guangdong Key Laboratory for New Technology Research of Vegetables, Vegetable Research Institute, Guangdong Academy of Agricultural Sciences, Guangzhou 510640, China
3. Jiangxi Provincial Key Laboratory of Ex Situ Plant Conservation and Utilization, Lushan Botanical Garden, Chinese Academy of Sciences, Jiangxi 332000, China
†These authors contributed equally to this work.
*Correspondences: Mingkun Huang (huangmk@lsbg.cn); Fanjiang Kong (kongfj@gzhu.edu.cn); and Zhihui Sun (szh@gzhu.edu.cn; Dr. Sun is fully responsible for the distribution of all materials associated with this article)

Jianhao Wang

Zhihui Sun

ABSTRACT

In plants, the photoperiod sensitivity directly influences flowering time, which in turn affects latitudinal adaptation and yield. However, research into the mechanisms underlying photoperiod sensitivity, particularly those mediated by epigenetic regulation, is still in its nascent stages. In this study, we analyzed the regulation of photoperiod sensitivity in *Arabidopsis thaliana*. We demonstrate that the evening complex LUX ARRYTHMO (LUX) and the chromatin remodeling factor SWITCH/SUCROSE NONFERMENTING 3C (SWI3C) regulate *GI* locus chromatin compaction and H3K4me3 modification levels at the *GIGANTEA* locus under different photoperiod conditions. This mechanism is one of the key factors that allow plants to distinguish between long-day and short-day photoperiods. Our study provides insight into how the LUX–SWI3C module regulates photoperiod sensitivity at the epigenetic level.

Keywords: chromatin remodeling, circadian clock, evening complex, histone modification, photoperiod sensitivity

Wang, J., Liu, H., Li, H., Wang, F., Yang, S., Yue, L., Liu, S., Liu, B., Huang, M., Kong, F., et al. (2025). The LUX–SWI3C module regulates photoperiod sensitivity in *Arabidopsis thaliana*. J. Integr. Plant Biol. **00:** 1–17.

INTRODUCTION

To ensure successful reproduction, plants must select the appropriate time to transition from vegetative growth to reproductive development. This transition is governed by the perception of various environmental cues, among which photoperiod—the length of day and night—plays a pivotal role in determining when to flower. Based on their responses to different day lengths, plants are categorized into long-day (LD), short-day (SD), and day-neutral species. Arabidopsis (*Arabidopsis thaliana)* is a typical facultative LD model plant, and its photoperiod-regulated flowering has been extensively studied (Song et al., 2015; Creux and Harmer, 2019; Takagi et al., 2023). Photoreceptors continuously detect changes in photoperiod and relay this information through a series of signaling events to GIGANTEA (GI), a critical regulatory component in the photoperiodic pathway (Yu et al., 2008; Shim et al., 2017; Liu et al., 2023). GI interacts with the F-BOX protein FLAVIN BINDING KELCH REPEAT F-BOX protein 1 (FKF1) to degrade the DOF family transcriptional regulators cyclic DOF factors (CDFs) (Imaizumi et al., 2005; Sawa et al., 2007), thereby alleviating the transcriptional repression of the core photoperiodic pathway factor gene *CONSTANS* (*CO*) (Fornara et al., 2009), whose encoded protein CO induces transcription of *flowering locus T* (*FT*) in the phloem (Samach et al., 2000; An et al., 2004; Wigge et al., 2005). FT is then transported to the shoot apical meristem (SAM), where it regulates the expression of a suite of flowering genes and promotes flowering (Corbesier et al., 2007).

The evening complex (EC) acts as a transcriptional repressor, binding to the promoters of key target genes and keeping their expression low (Nusinow et al., 2011). The EC primarily consists of EARLY FLOWERING 3 (ELF3), ELF4, and LUX ARRHYTHMO (LUX, reported as PHYTOCLOCK1 (PCL1)), with all of the encoding genes showing peak expression at dusk. LUX is a MYB family transcription factor (Silva et al., 2016), ELF4 is a small nucleus-localized protein that promotes the nuclear localization of ELF3 (Doyle et al., 2002; Kikis et al., 2005; Huang et al., 2016), and ELF3 interfaces with ELF4 and LUX, connecting the EC to light-signaling pathways through its interactions with phytochrome B (phyB) and CONSTITUTIVELY PHOTOMORPHOGENIC1 (COP1), ELF3 also acts as a temperature sensor through a prion-like domain (Liu et al., 2001; Yu et al., 2008; Jung et al., 2020), thus conferring temperature-dependent genome-wide targeting capability to the EC. Located in the cell nucleus, the EC inhibits the expression of key circadian genes such as *TIMING OF CAB EXPRESSION 1 (TOC1), LUX, GI, and PSEUDO-RESPONSE REGULATOR 7 (PRR7)* and *PRR9*, indirectly promoting the expression of the morning oscillator component *CIRCADIAN CLOCK ASSOCIATED 1 (CCA1)* and *LATE ELONGATED HYPOCOTYL* (*LHY*) (Nusinow et al., 2011; Herrero and Davis, 2012; Ezer et al., 2017).

In eukaryotic organisms, DNA replication, DNA repair, and transcription typically require a relaxed chromatin state. However, the tight winding of DNA around histone octamers hinders access by various regulatory proteins. Chromatin remodeling has evolved as a mechanism that addresses this issue. Chromatin remodeling factors slide, remove, or replace nucleosomes at specific sites through ATP hydrolysis, altering the chromatin structure, thereby facilitating transcription and playing a crucial role in biological programs such as cell differentiation, development, and DNA repair (Clapier et al.,2017). Chromatin remodeling is often associated with cross-talk with histone modifications (Li et al., 2016b; Guo et al., 2022; Fu et al., 2023). SWITCH/SUCROSE NONFERMENTING 3C (SWI3C), a chromatin remodeling factor, is a key subunit of the Arabidopsis switch defective/sucrose non-fermentable (SWI/SNF) complex (BRM-associated SWI/SNF complexes), overlapping in function with the core subunit BRAHMA (BRM). The *swi3c* mutants usually exhibit phenotypes such as growth retardation, impaired root development, leaf curling, abnormal stamens, and lower fertility (Sarnowski et al., 2005; Archacki et al., 2009). Current research on SWI3C remains limited, but it is known to affect the transcription of *FLOWERING LOCUS C* (*FLC*), as well as participate in flowering regulation and the gibberellin pathway in Arabidopsis (Sarnowski et al., 2005; Sarnowska et al., 2013).

Previous reports have shown that the EC plays a central role in photoperiodic flowering in Arabidopsis, rice (*Oryza sativa*), maize (*Zea mays*), pea (*Pisum sativum*), and soybean (*Glycine max*) (Liew et al., 2009; Weller and Ortega, 2015; Li et al., 2016b; Lu et al., 2017; Bu et al., 2021; Andrade et al., 2022). However, EC target genes vary between species. For instance, in *Arabidopsis*, LUX can form a complex with HIGH EXPRESSION OF OSMOTICALLY RESPONSIVE GENES 15 (HOS15) and HISTONE DEACETYLASE 9 (HDA9) that regulates *GI* expression (Park et al., 2019) while, in rice, LUX affects photoperiodic flowering by regulating the transcription of *PRR37* and *Grain number, plant height, and heading date7* (*Ghd7*) (Andrade et al., 2022). In the model SD crop soybeans, LUX directly binds to the promoter of the key flowering gene *E1* and inhibits its expression (Bu et al., 2021). In our recent study, we demonstrated that the soybean GI homolog E2 forms a feedback loop with the EC, with E2 forming a complex with FKF1 that degrades the soybean ELF3 homolog J, while the EC simultaneously suppresses *E2* transcription. This antagonistic and mutually regulatory cycle established between E2 and EC determines soybean photoperiod sensitivity (Zhao et al., 2024). However, the mechanisms by which the EC regulates photoperiod sensitivity in LD plants, such as in Arabidopsis, remain unclear. In this study, through an analysis of photoperiod sensitivity in Arabidopsis, we discovered that the LUX–SWI3C module mediates photoperiod sensitivity through the epigenetic regulation of *GI*. When this module is impaired, Arabidopsis cannot effectively distinguish between LD and SD conditions, displaying an extreme early-flowering phenotype indicative of a loss of photoperiod sensitivity. Our findings reveal that the LUX–SWI3C module epigenetically regulates *GI* transcription, constituting one of the pathways that regulate photoperiod sensitivity in the LD plant Arabidopsis.

RESULTS

Evening complex components regulate photoperiod sensitivity in Arabidopsis

Photoperiod sensitivity plays a crucial role in the recognition of different photoperiods, thus guiding the timing of flowering. A change in flowering time when plants are grown under different photoperiods is a critical outward manifestation of plant photoperiod sensitivity. To elucidate the molecular mechanisms regulating photoperiod sensitivity in Arabidopsis, we wished to identify the key factor(s) that govern this response. Mutations in the genes encoding such factors would be expected to cause a loss of photoperiod sensitivity. Given that our previous work had demonstrated a significant role for the EC in photoperiod sensitivity in the SD plant soybean (Zhao et al., 2024), we investigated the flowering time of Arabidopsis mutants in individual EC components. We determined that the mutants *lux6*, *elf3-1*, and *elf4-209*, defective in LUX, ELF3, and ELF4, respectively, show extreme insensitivity to photoperiod, as evidenced by their very early flowering under both LD (16-h light/8-h dark) and SD (8-h light/16-h dark) conditions, producing only about seven rosette leaves before flowering, consistent with previous reports (Hazen et al., 2005) (Figure 1A, B). These findings clearly indicate that the EC in Arabidopsis is also involved in photoperiod sensitivity.

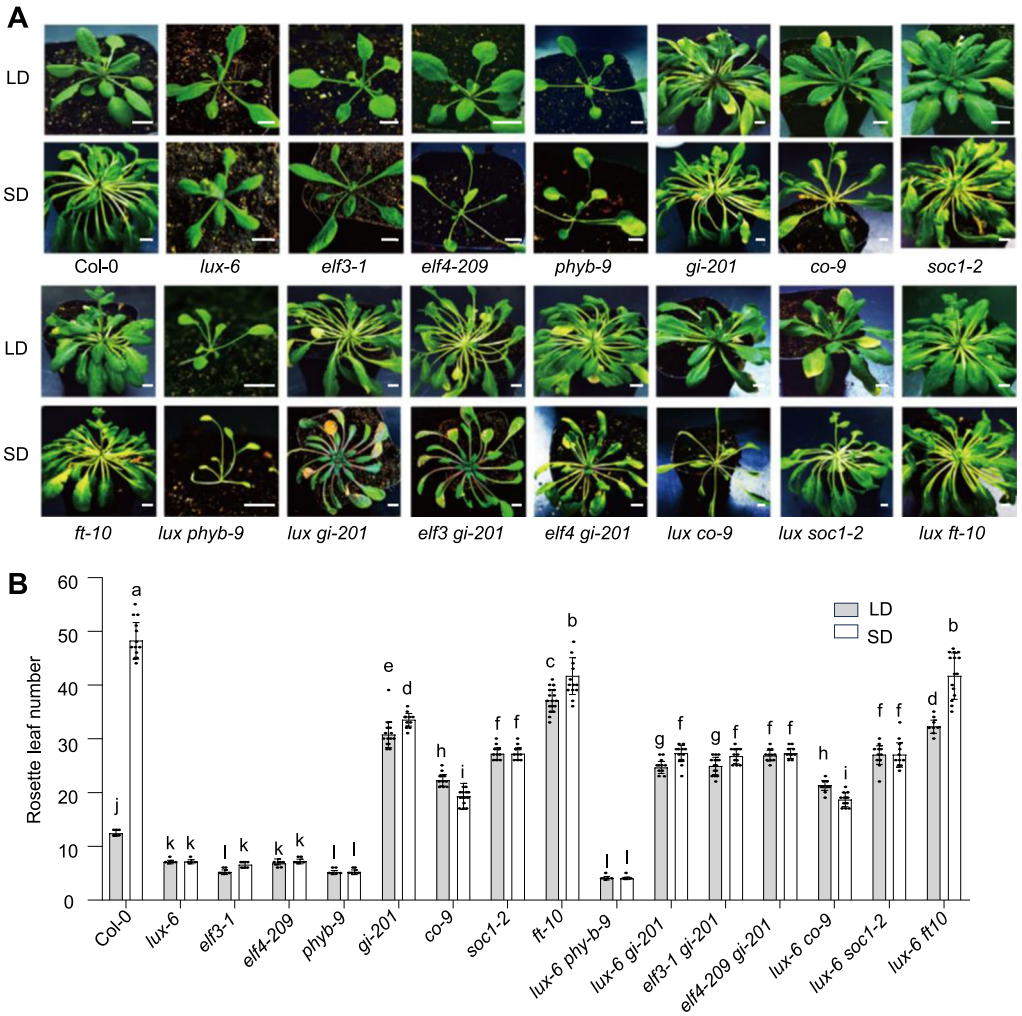

Figure 1. Analysis of the genetic relationship between evening complex (EC) genes and primary flowering regulatory genes
(A) Representative photographs of wild-type (Col-0) and EC mutants *(lux-6*, *elf3-1*, and *elf4-209*), key floral regulatory gene mutants (*phyb-9*, *co-9*, *gi-201*, *soc1-2*, and *ft-10*), and several double mutants. Plants were grown under long-day (LD; 16-h light/8-h dark) or short-day (SD; 8-h light/16-h dark) conditions until the onset of flowering (when the flowering stem was 1 cm in height Scale bar, 1 cm), when the number of rosette leaves was determined. **(B)** Number of rosette leaves at the time of flowering for the genotypes shown in **(A)**. For each biological replicate, about 20 plants for each genotype were scored per photoperiod condition, with three biological replicates carried out with consistent results. Values are means ± *SD*, with individual data points from one representative biological replicate shown as black dots. Different lowercase letters indicate a significant difference at $P < 0.05$ based on one-way analysis of variance (ANOVA).

To genetically dissect the role of LUX in the regulation of photoperiod sensitivity, we generated several double mutants consisting of *lux-6* and mutants of key floral regulatory genes and examined their flowering behaviors by counting the number of rosette leaf numbers under SD and LD conditions. The *lux-6 gi-201* double mutant exhibited a flowering phenotype with a leaf number intermediate between that of *lux-6* and *gi-201*, although closer to *gi-201*. This suggests that LUX functions genetically largely upstream of *GI*. However, the incomplete similarity to the *gi-201* phenotype in the double mutant may indicate that LUX also regulates other downstream targets, such as *PRR7* and *PRR9*. The double mutants *lux-6 co-9*, *lux-6 soc1-2*, and *lux-6 ft-10* flowered at the same time as the corresponding *co-9*, *soc1-2*, and *ft-10* single mutants, indicating that *LUX* is genetically located upstream of *CO*, *SOC1*, and *FT*. Similarly, double mutants consisting of *gi-201* and mutants of other EC members, *elf3-1* and *elf4-209*, displayed flowering times comparable with *gi-201*, suggesting they are also genetically upstream of *GI*. By contrast, the *lux-6 phyb-9* double mutant flowered at the same time as the *phyb-9* single mutant, suggesting that *LUX* and *PHYB* may function at the same genetic level, or that they may act independently. As the EC component ELF3 forms a complex with phyB (Huang et al., 2016; Kwon et al., 2024), we suggest that *PHYB* may act together with *LUX* in the same genetic pathway. When performing a one-way analysis of variance (ANOVA) on the data, the difference between *phyb-9* and *lux-6* appears small in Figure 1B, probably because other genotypes display greater differences from these mutants. However, when we performed a

separate *t*-test analysis focusing on the *phyb-9* and *lux-6 phyb-9* mutants, we detected significant differences under both SD and LD conditions ($P < 0.001$). Additionally, the *lux-6 phyb-9* double mutant flowered earlier than the *lux-6* and *phyb-9* single mutants. (Figure 1A, B). Overall, we conclude that the EC complex plays a crucial role in regulating photoperiod sensitivity, with *LUX* located upstream of *GI*, *CO*, *SOC1*, and *FT* in the genetic hierarchy.

LUX physically interacts with SWI3C and both are genetically dependent on *GI*

LUX was previously reported to form complexes with HOS15 and HDA9 that regulate the photoperiodic flowering pathway specifically under LD conditions (Park et al., 2019). In this study, we focused on the role of *LUX* in photoperiod sensitivity, specifically in the recognition of LD and SD conditions. Therefore, the complex formed by HDA9 and HOS15 with EC might not be sufficient to explain this phenomenon. To dissect the molecular mechanisms by which LUX regulates photoperiod sensitivity, we looked for protein(s) that interact with LUX and whose mutation results in a loss of photoperiod sensitivity. We thus conducted a yeast-two-hybrid (Y2H) library screening and identified the critical subunit SWI3C of the SWI/SNF chromatin remodeling complex as a candidate interactor. To validate the authenticity of this interaction, we conducted a targeted Y2H assay, co-transforming the constructs LUX–AD (a fusion between LUX and the activation domain (AD) of yeast GAL4) and SWI3C–BD (a fusion of SWI3C and the DNA-binding domain (BD) of yeast GAL4) into yeast cells. The growth of positive transformants on a synthetic defined medium lacking leucine, tryptophan, histidine, and adenine confirmed their interaction in yeast (Figure S1A). We also tested the interaction between SWI3C and two other key components of the EC, ELF3, and ELF4, but detected no interaction. As ELF3 and ELF4 are crucial for gating of light responses to the circadian clock in the LUX–ELF3–ELF4 protein complex, we asked whether ELF3 and/or ELF4 might influence the interaction between LUX and SWI3C. We examined this question in a yeast-three-hybrid assay (Y3H) (Figure S1B), co-transforming AD–SWI3C with pBridge–LUX–ELF3 or pBridge–LUX–ELF4 and measuring the resulting β-galactosidase activity, using yeast cells co-transformed with AD–SWI3C and pBridge–LUX alone as the control. We observed no significant differences in β-galactosidase activity for the LUX–SWI3C interaction regardless of ELF3 or ELF4 presence or absence suggesting that ELF3 and ELF4 do not influence the strength of the LUX–SWI3C interaction in the Y3H system. Luciferase complementation imaging (LCI) and bimolecular fluorescence complementation (BiFC) assays indicated that LUX interacts with SWI3C *in vivo* when the appropriate constructs are co-infiltrated into the leaves of *Nicotiana benthamiana* plants and that this interaction occurs in the nucleus (Figure 2A, B). We verified the interaction between LUX and SWI3C in an *in vitro* glutathione *S*-transferase (GST) pull-down assay, using recombinant purified GST-LUX and HIS-SWI3C (Figure 2C). To assess their *in vivo* interaction, we generated the transgenic complementation line *pSWI3C*:SWI3C-GFP/*swi3c-3* (Figure S2A–C), following immunoprecipitation with an anti-GFP antibody, we detected LUX in the immunoprecipitates, confirming their interaction *in vivo* (Figures 2D, S1). Taken together, these results suggest that LUX and SWI3C interact both *in vitro* and *in vivo*, suggesting that SWI3C may co-regulate photoperiod sensitivity alongside LUX.

Before investigating whether and how LUX and SWI3C co-regulate photoperiod sensitivity, we checked their protein levels in seedlings grown under LD and SD conditions. To this end, we conducted an immunoblot analysis of LUX protein abundance in 14-d-old Col-0 seedlings grown under SD or LD conditions using a commercial anti-LUX antibody. LUX protein levels did not show significant changes under LD and SD conditions at any time point across the diurnal cycle, suggesting that LUX abundance is not sensitive to photoperiod changes (Figure S3A–C). We also tested SWI3C protein levels in the *proSWI3C*:*SWI3C-GFP*/*swi3c-3* transgenic line. SWI3C protein abundance, as determined with an anti-GFP antibody, followed the same pattern in seedlings grown under SD and LD conditions, indicating that SWI3C abundance is not affected by photoperiod (Figure S3D, E).

Aside from their protein levels, the interaction strength between LUX and SWI3C may also influence their response to photoperiod regulation. To assess for a possible difference in the LUX–SWI3C interaction under SD and LD conditions, we performed co-immunoprecipitation (co-IP) experiments using total protein extracted from 14-d-old *proSWI3C:SWI3C-GFP*/*swi3c-3* and pSuper:*GFP* seedlings grown under SD or LD conditions. The amount of LUX co-immunoprecipitated with SWI3C was higher in seedlings grown under SD conditions than from those grown under LD conditions (Figures 2D, S1C). This result indicates that the LUX–SWI3C interaction strength is indeed sensitive to photoperiod, with a weaker interaction under LD conditions.

Although LUX and SWI3C interact, evidence supporting their joint regulation of photoperiod sensitivity is lacking. To establish their co-regulatory role, two prerequisites must be met: (i) they interact; and (ii) there is a loss of photoperiod sensitivity in Arabidopsis upon mutation of *SWI3C*. We therefore obtained a T-DNA insertion mutant for *SWI3C* and characterized its flowering time when grown under LD or SD conditions. Importantly, the *swi3c-3* and *lux-6* single mutants exhibited similar early-flowering phenotypes, with about seven rosette leaves at the time of flowering, significantly fewer than for the wild-type Col-0 (Figure 2E–G). We observed a similar phenotype in another *swi3c* mutant line, *swi3c-2*, suggesting that *SWI3C* is indeed involved in the regulation of photoperiod sensitivity, the photoperiod sensitivity phenotype of *swi3c-2* was not completely abolished compared with that of *swi3c-3*. Additionally, we evaluated the photoperiod sensitivity of the complementation line *proSWI3C*:SWI3C-GFP/*swi3c-3*, demonstrating substantial rescue of the *swi3c-3* mutant phenotype (Figure S2A–C). LUX may therefore interact with SWI3C to co-regulate photoperiod sensitivity.

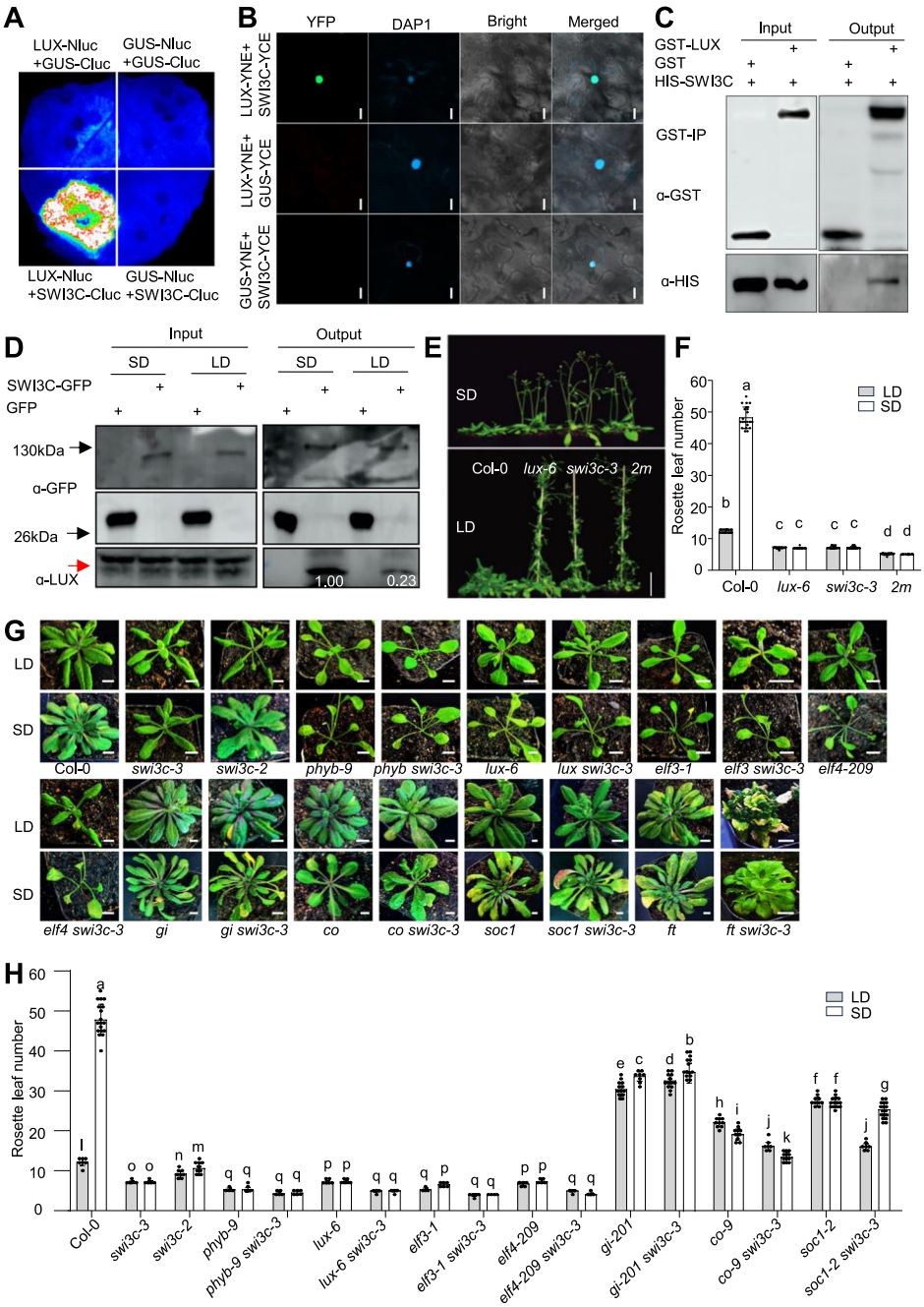

Figure 2. Interaction between LUX and SWI3C and their genetic relationship

(A) Luciferase complementation imaging (LCI) assay showing that LUX interacts with SWI3C. **(B)** Bimolecular fluorescence complementation (BiFC) analysis of the interaction between LUX and SWI3C. Scale bars, 20 μm. **(C)** Glutathione *S*-transferase (GST) pull-down assay showing that LUX interacts with SWI3C *in vitro*. Proteins were detected with anti-GST and anti-HIS antibodies. **(D)** Co-immunoprecipitation (Co-IP) assay demonstrating the interaction between LUX and SWI3C-GFP in Arabidopsis 14-d-old *35S:GFP* and p*roSWI3C:SWI3C-GFP*/*swi3c-3* seedlings grown under short-day (SD) or long-day (LD) conditions. LUX abundance in SD-grown seedlings was set to 1. Immunoblotting was performed with anti-GFP (top two rows) and anti-LUX (bottom row) antibodies. **(E)** Representative photographs of Col-0, *lux-6*, *swi3c-3*, and the *lux-6 swi3c-3* double mutant (*2m* in the figure). Plants were grown under LD or SD conditions until the onset of flowering. Scale bar, 5 cm. **(F)** Number of rosette leaves at flowering for the genotypes shown in **(E)**. For each biological replicate, about 20 plants per genotype and condition were scored, with three biological replicates, each showing consistent results. Values are means ± *SD*, with individual data points from one representative biological replicate shown as black dots. Different lowercase letters indicate a significant difference at $P < 0.05$ based on one-way ANOVA. **(G)** Representative photographs of Col-0, *swi3c-3* and *swi3c-2* single mutants, key floral regulatory mutants (*phyb-9*, *co-9*, *gi-201*, *soc1-2*, *ft-10*), and their respective double mutants with *swi3c-3* at the onset of flowering. Scale bar, 1 cm. **(H)** Number of rosette leaves at flowering for the genotypes shown in **(G)**. For each biological replicate, about 20 plants per genotype and condition were scored, with three biological replicates, each showing consistent results. Values are means ± *SD*, with individual data points from one representative biological replicate shown as black circles. Different lowercase letters indicate a significant difference at $P < 0.05$ based on one-way ANOVA.

To support our hypothesis, we analyzed the genetic relationship between *LUX* and *SWI3C* by generating the *lux-6 swi3c-3* double mutants. While the two single mutants were already insensitive to photoperiod, the double mutants displayed an additive effect, losing photoperiod sensitivity and exhibiting an even earlier flowering phenotype with only about five rosette leaves, suggesting that LUX and SW13C may control photoperiod sensitivity at the same regulatory level or within independent regulatory pathways (Figure 2D, F). As SWI3C also regulated photoperiod sensitivity, we crossed *swi3c-3* to mutants in key flowering genes (*phyb-9, gi-201, co-9, soc1-2, ft-10*) and obtained the corresponding double mutants. The *gi-201 swi3c-3* double mutant flowered at a time very similar to *gi-201*, indicating that SWI3C genetically acts upstream of *GI*. However, the *co-9 swi3c-3* and *soc1-2 swi3c-3* double mutants occasionally flowered at a time between *co-9* or *soc1-2* and *swi3c-3* under both LD and SD conditions, suggesting that SWI3C acts upstream of CO and SOC1, but may also regulate other downstream genes. Interestingly, most *ft-10 swi3c-3* double-mutant plants failed to flower under LD conditions and showed pronounced developmental defects (Figure 2G). Furthermore, the *elf3-1 swi3c-3* and *elf4-209 swi3c-3* double mutants were fully photoperiod insensitive and flowered slightly earlier than the *elf3-1* and *elf4-209* single mutants, similar to *lux-6 swi3c* (Figure 2G, H). In summary, SWI3C and the EC regulate photoperiodic flowering at the same genetic level or are involved in different regulatory pathways, with both SWI3C and LUX located upstream of the key flowering component GI.

LUX and SWI3C regulate photoperiod sensitivity by influencing *GI* transcription

We hypothesized that LUX and SWI3C operate at the same regulatory level. A previous report demonstrated that the HOS15–EC–HDA9 complex regulates flowering under LD conditions by inhibiting the transcription of *GI* (Park et al., 2019). As *LUX* and *SWI3C* acted genetically upstream of *GI* under both LD and SD conditions (Figure 2G, H), we speculated that LUX and SWI3C may jointly regulate *GI* expression and regulate photoperiod sensitivity. To test this idea, we examined the expression patterns of key flowering genes in 14-d-old Col-0, *lux-6*, *swi3c-3*, and the *lux-6 swi3c-3* (*2m*) double-mutant seedlings grown under LD or SD conditions by reverse transcription quantitative PCR (RT-qPCR) analysis. *GI* expression levels were significantly lower under SD conditions than under LD conditions, indicating that photoperiod affects *GI* expression in the wild-type (Figure S3F; Table S3). Regardless of the photoperiod, *GI* transcript levels in *lux-6* and *swi3c-3* seedlings were significantly higher than those in the wild-type, especially after the light-to-dark transition. Additionally, *GI* was expressed at higher levels in the *lux6 swi3c-3* double mutant than in the *lux6* and *swi3c-3* single mutants, consistent with our genetic analysis and indicating an additive effect (Figure 3A, B; Table S3). We also measured the expression levels of *CO*, *SOC1*, and *FT* in the same seedlings (Figure S4A–F). Under both LD and SD conditions, *CO* expression levels were higher in the single and double mutants than in the wild-type. *SOC1* expression in *lux-6* and *swi3c-3* exhibited a pattern distinct from that seen with *GI*, suggesting that LUX and SWI3C may regulate *SOC1* expression through different pathways. Notably, *FT* expression markedly changed between SD and LD conditions. Under SD conditions, *FT* expression in *lux-6* was higher than in Col-0 for most of the day, except at ZT24, when it was lower. In *swi3c-3*, *FT* expression was only higher than that in Col-0 around ZT4. In the *lux-6 swi3c-3* double mutants, *FT* expression did not show a clear additive effect. Under LD conditions at ZT16, *swi3c-3* and the *lux6 swi3c-3* double mutants expressed FT at higher levels than Col-0 and *lux-6*, with *FT* expression levels in Col-0 and *lux-6* being similar. These observations suggest that LUX and SWI3C may regulate *FT* expression independently. Furthermore, the differences seen in the mutants in terms of *FT* expression under LD and SD conditions indicate that these effects may not be related to the photoperiod sensitivity regulation under investigation in this study (Figure S4A–F). Taken together, the genetic and gene expression analyses suggest that LUX and SWI3C regulate *GI* transcript levels, thereby contributing to the regulation of photoperiod sensitivity. The comparable effects on gene expression levels by the *swi3c-3* and *lux6* mutants are in agreement with previous genetic analysis (Figure 2F), indicating the possibility that LUX and SWI3C operate at the same regulatory level.

LUX–SWI3C regulates chromatin compaction and H3K4me3 levels at the *GI* locus

To ascertain whether *GI* is the main target gene through which LUX and SWI3C jointly regulate photoperiod sensitivity, we asked whether they bind to the *GI* locus and explored the histone modification landscape over *GI* in wild-type and mutants using previously published chromatin immunoprecipitation sequencing (ChIP-seq) data (Ezer et al., 2017; Guo et al., 2022; Zhao et al., 2022). Among the 831 genes to which LUX binds, 153 were also bound by SWI3C (Figure 3C; Table S1). Notably, at well annotated genes such as *GI*, *LUX*, and *PRR7*, the binding sites for LUX and SWI3C were nearly identical (Figures 3D, S5A–C). Given the association of the SWI/SNF complex with histone modifications such as H3K27me3, H3K4me3, and H3ac (Li et al., 2016a; Guo et al., 2022; Fu et al., 2023), we analyzed ChIP-seq data for these histone marks on several genes (*GI*, *LUX, PRR7*, *PRR9*) in Col-0. We detected a notable enrichment of H3K4me3, H3K9ac, and H3K27ac marks over the promoters of *GI*, while H3K27me3 was not enriched along the *GI* gene body (Figure 3D). Of note, the ChIP-seq data analyzed here were derived from seedlings grown under LD conditions, where LUX and SWI3C probably bind to the *GI* locus, potentially altering its histone modification status. These data alone are insufficient to conclude that LUX and SWI3C can regulate photoperiod sensitivity through *GI* expression. To gain deeper insights into whether and how LUX and SWI3C regulate *GI* expression and control photoperiod sensitivity, and to validate the published ChIP-seq results, we

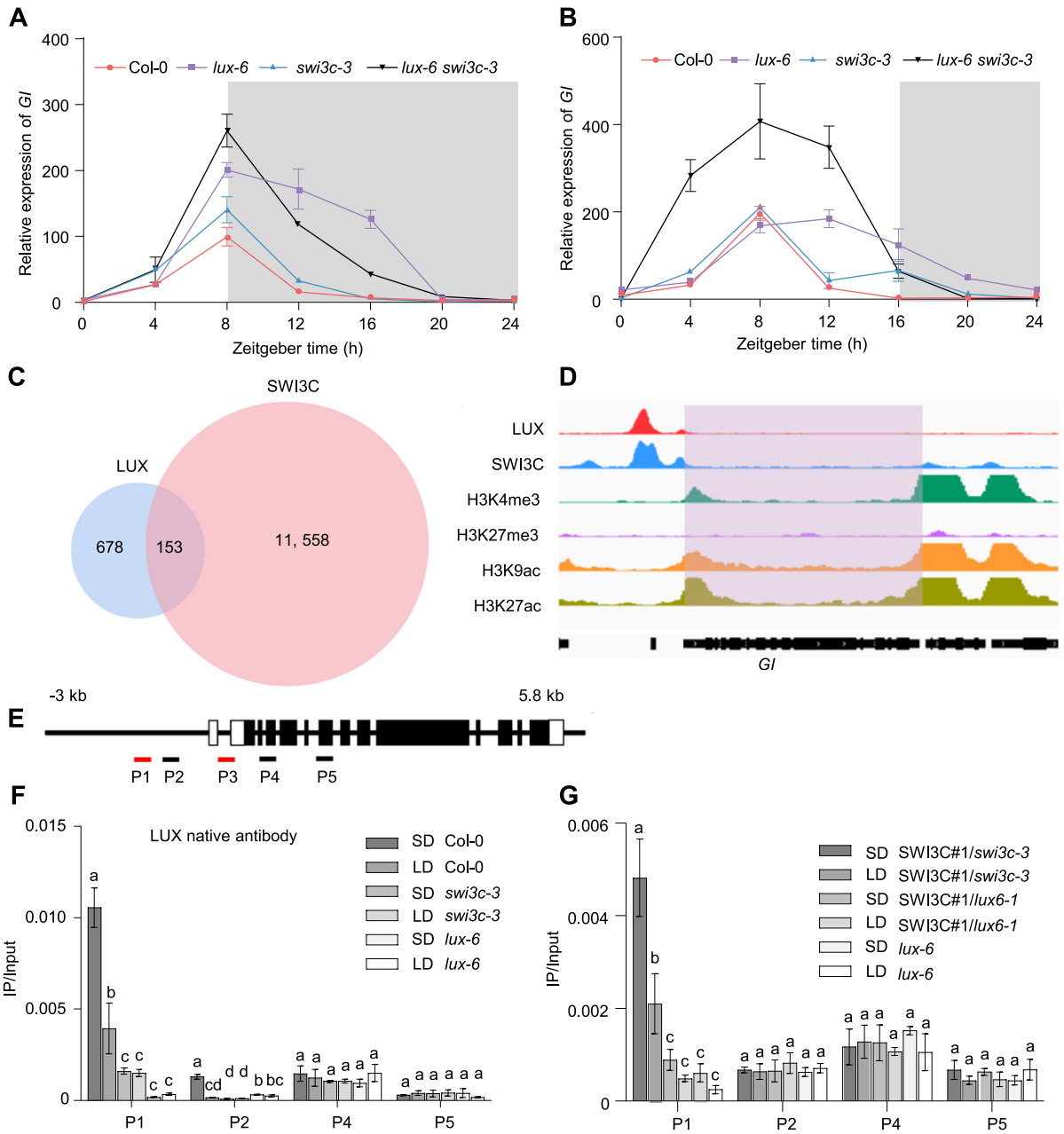

Figure 3. LUX and SWI3C regulate photoperiod sensitivity by *GI* transcript levels

(A, B) Relative *GI* transcript levels in Col-0, *lux-6*, *swi3c-3*, and *lux-6 swi3c-3* (2 *m*) 14-d-old seedlings grown under short-day (SD) **(A)** or long-day (LD) **(B)** conditions. Total RNA was extracted from samples collected at zeitgeber times ZT0, ZT4, ZT8, ZT12, ZT16, ZT20, and ZT24. UBQ10 was used as the internal reference gene. Each biological replicate consisted of three technical replicates, with one representative biological replicate shown. Values are means ± *SD* from three independent biological replicates. *P*-values were obtained using a two-sided Student's *t*-test; ns, no significant difference; $^{*}P < 0.05$, and $^{**}P < 0.01$. The statistical analyses are shown in Table S3. **(C)** Venn diagram showing the extent of overlap for the number of genes bound by LUX or SWI3C. **(D)** Integrative Genome Viewer (IGV) visualization of LUX and SWI3C binding sites across the *GI* genomic region, alongside enrichment of histone modifications at this locus in Col-0. **(E)** Diagram of the GI locus illustrating the PCR amplicons containing LUX-binding motifs, denoted by red lines, and PCR amplicons without such motifs, indicated by black lines. The white rectangles represent untranslated regions, the black rectangles denote exon regions, and the black lines represent either intron or promoter regions. **(F)** Quantification of LUX binding at the GI locus. Here, 14-d-old seedlings were harvested at the transition from light to dark (ZT8 for SD conditions; ZT16 for LD conditions). Chromatin immunoprecipitation assays used anti-LUX antibodies, and the bound DNA was quantified by quantitative PCR (qPCR). The average IP data were normalized to total input DNA. Values are means ± *SD* from three biological replicates. Different lowercase letters indicate a significant difference at $P < 0.05$, as determined by multiple comparison testing by one-way ANOVA. **(G)** Quantification of SWI3C binding to the *GI* locus in 14-d-old *lux-6*, *proSWI3C:SWI3C-GFP* #1/*lux-6*, and *proSWI3C:SWI3C-GFP* #1/*swi3c-3* seedlings collected at the transition from light to dark (ZT8 for SD conditions; ZT16 for LD conditions). Chromatin immunoprecipitation assays were performed with anti-GFP antibodies, and the bound DNA was quantified by qPCR. The average IP data were normalized to total input DNA. Values are means ± *SD* from three biological replicates. Different lowercase letters indicate a significant difference at $P < 0.05$, as determined by multiple comparison testing by one-way ANOVA.

used a commercially available anti-LUX antibody for ChIP-qPCR analysis of LUX binding to the *GI* locus, with PCR amplicons targeting two regions containing a LUX-binding site (LBS, GATWCG motif, where W is A or T; Sites 1 and 3) and three regions lacking an LBS (Sites 2, 4, and 5). As LUX and SWI3C abundance was higher around the light–dark transitions under LD and SD conditions, we selected these time points for ChIP-qPCR analysis (Figure S3B–E). We observed significant enrichment of LUX at Site 1 under both LD and SD conditions; but no binding of LUX was detected at site 3 (Figure 3E, F). Similarly, in the *proSWI3C*:SWI3C-GFP/*swi3c-3* lines, we detected a significant enrichment for SWI3C at Site 1 under both LD and SD conditions (Figure 3G). As we hypothesized that LUX and SWI3C regulate photoperiod sensitivity by controlling *GI* expression, we compared the binding abilities of LUX and SWI3C to the *GI* locus in Col-0 and *proSWI3C:*SWI3C-GFP/*swi3c-3* under both LD and SD conditions. The binding of LUX and SWI3C to site 1 of the *GI* locus is higher under SD conditions than under LD conditions (Figure 3F, G). This finding aligns with our observation of a stronger LUX–SWI3C interaction intensity under SD conditions (Figures 2D, S3A–C). These results demonstrate that both LUX and SWI3C participate in the regulation of photoperiod sensitivity by binding to the *GI* locus.

Although both LUX and SWI3C bind to the *GI* promoter, the above genetic analysis (Figure 2E–H) alone is not sufficient to conclude that they regulate photoperiod sensitivity by cooperatively controlling *GI* transcription at the same regulatory level. Indeed, they may independently regulate *GI* expression. Thus, to delineate the extent of interdependence between LUX and SWI3C, we measured the LUX enrichment at the *GI* sites in the *swi3c-3* mutant and the SWI3C enrichment at the *GI* sites in *proSWI3C*:SWI3C-GFP/*lux-6* under SD and LD conditions. Importantly, the ChIP-qPCR signal in these genetic backgrounds was similar to that of the negative control *lux-6*, indicating the mutual dependence of LUX and SWI3C for binding to the *GI* promoter (Figure 3F, G). This finding corroborates our earlier genetic analysis (Figure 2E–H), suggesting that LUX and SWI3C interdependently regulate photoperiod sensitivity through controlling *GI* transcription, aligning with our initial hypothesis. This interdependence may be due to LUX recognizing its cognate binding site, after which SWI3C would be recruited to alter the nearby epigenetic landscape.

To test this hypothesis, considering that SWI3C is a subunit of the SWI/SNF chromatin remodeling complex, we used micrococcal nuclease (MNase)-qPCR assays to assess nucleosome occupancy at the *GI* locus. The MNase-qPCR analysis showed that chromatin at the *GI* locus is more relaxed in the *lux-6* and *swi3c-3* mutants than in the wild-type. In the *lux-6 swi3c-3* double mutant, the chromatin at the *GI* locus appeared even more relaxed under SD conditions, consistent with our genetic and gene expression findings (Figure 4A). We observed largely comparable chromatin relaxation in the single and double mutants under LD conditions (Figure 4B). SWI/SNF complexes are often associated with histone modifications such as H3K27me3, H3K4me3, and H3K9ac, and both histone modifications and chromatin relaxation levels directly influence transcription. Therefore, we evaluated the levels of these modifications at the *GI* locus in 14-d-old Col-0, *lux-6*, *swi3c-3*, and *lux-6 swi3c-3* seedlings grown under LD and SD conditions. The levels of the H3K4me3 modification at Sites 3 and 4 significantly rose with the loss of *LUX* and/or *SWI3C*, regardless of photoperiod (Figure 4C, E). Additionally, in the wild-type, H3K4me3 levels at Sites 3 and 4 were higher under LD conditions than under SD conditions, further indicating that *GI* expression is likely to be regulated by LUX-SWI3C in response to photoperiod sensitivity (Figure 4F). This finding is consistent with our RT-qPCR analysis (Figure S3F). The enrichment of H3K27me3 at the *GI* locus was minimal, with only Sites 3 and 4 showing weak signals, and with little difference between the mutants and the wild-type; no signals were detected at other sites (Figure S6A–C). We also assessed the enrichment of H3ac at the *GI* locus, obtaining results that were in line with previous reports (Park et al., 2019). Under LD conditions, the level of H3ac enrichment was significantly higher in the *lux-6* mutant than in Col-0 (Park et al., 2019). However, there was little to no change in the enrichment degree of H3ac at the *GI* locus between the *swi3c-3* mutant and Col-0 under both LD and SD conditions. We conclude that SWI3C, unlike LUX, does not participate in the regulation of H3ac deposition at the *GI* locus. Furthermore, the H3ac enrichment at the *GI* locus did not appear to be strongly associated with photoperiod sensitivity (Figure S6D–F). SWI3C appears to be involved solely in the regulation of H3K4me3. The above results echo the mechanism observed for the regulation of the *SOC1* locus by BRM, as H3K27me3 levels also remain unchanged (Yang et al., 2022). Intricate cross-talk exists in epigenetic regulation, as chromatin remodeling factors lack histone-modifying activity. The regulation of H3K4me3 and H3ac deposition may involve the formation of more higher-order complexes with histone demethylases and histone deacetylases. Identifying the specific proteins directly involved in the direct regulation of H3K4me3 and H3ac deposition will be a focal point for our upcoming research efforts. As H3K4me3 is typically associated with transcriptional activation, we propose that the repression of *GI* by LUX and SWI3C is primarily due to the chromatin compaction they exert at the *GI* locus and to alterations in the levels of H3K4me3.

While we demonstrated here that the LUX–SWI3C module regulates *GI* transcription through epigenetic modulation, the ELF3 component of the EC can also regulate GI protein stability (Yu et al., 2008), raising the question whether the LUX–SWI3C module might also influence GI stability in addition to its role in transcriptional regulation. To investigate this point, we performed *in vitro* cell-free degradation assay by adding recombinant purified maltose-binding protein (MBP)-GI to total proteins extracted from Col-0, *lux-6*, *swi3c-3*, and *lux-6 swi3c-3*. Using protein extracts from seedlings grown under LD or SD conditions, recombinant MBP-GI exhibited a similar degradation profile regardless of the genotype (Figure S7A–D). These findings indicated that the

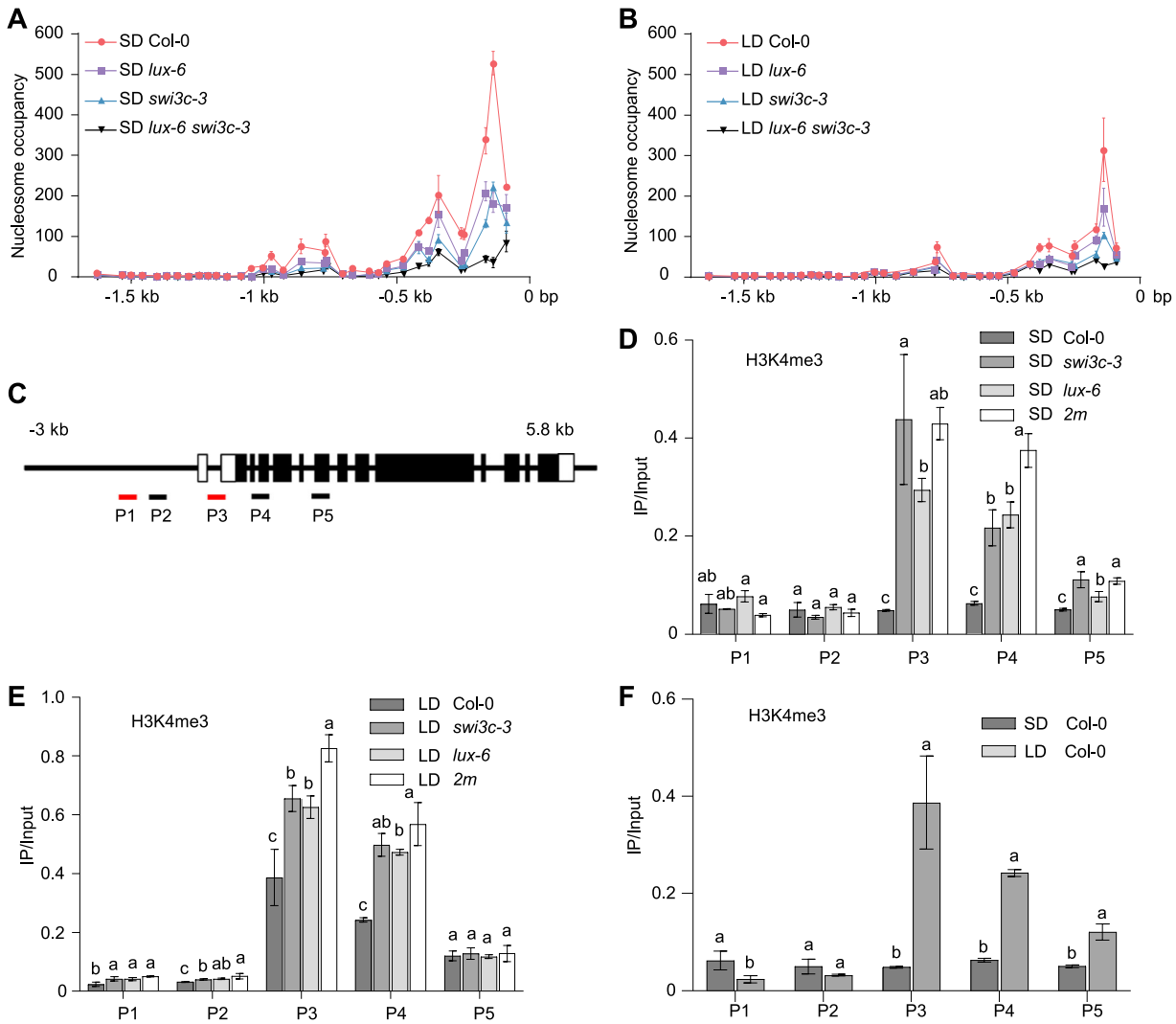

Figure 4. The LUX–SWI3C module regulates the chromatin compaction and H3K4me3 levels at the *GI* locus

(A, B) Nucleosome occupancy over the *GI* locus in Col-0, *lux-6*, *swi3c-3*, and *lux-6 swi3c-3* (*2m*) 14-d-old seedlings grown under short-day (SD) **(A)** or long-day (LD) **(B)** conditions, as analyzed by micrococcal ribonuclease (MNase)-qPCR. Seedlings were collected at the transition from light to dark. Values are means ± *SE* from three technical replicates, with the numbers on the *x*-axis representing the distance from the transcription start site (+1 bp); the numbers on the *y*-axis are as described in the Materials and Methods section and represent nucleosome occupancy. **(C)** Diagram of the *GI* locus illustrating the PCR amplicons containing LUX-binding motifs, denoted by red lines, and PCR amplicons without such motifs, indicated by black lines. **(D–F)** Quantification of H3K4me3 enrichment at the *GI* locus in 14-d-old Col-0, *lux-6*, *swi3c-3*, and *2m* seedlings grown under SD or LD conditions. Seedlings were collected at the transition from light to dark. Chromatin immunoprecipitation assays used anti-H3K4me3 antibodies, and the bound DNA was quantified by qPCR. The average IP data were normalized to total input DNA. Values are means ± *SD* from three biological replicates. Different lowercase letters indicate a significant difference at $P < 0.05$, as determined by multiple comparison testing by one-way ANOVA.

LUX–SWI3C module does not influence GI protein stability in this *in vitro* cell-free system. However, the results from cell-free degradation assays may not fully reflect GI protein dynamics *in vivo*, which warrants further investigation using anti-GI antibodies or transgenic materials.

DISCUSSION

To ensure successful reproduction, plants must flower at the appropriate time, completing the transition from vegetative growth to reproductive development (Liu et al., 2023). Photoperiod is a critical environmental factor influencing flowering time, as first discovered by Garner and Allard in 1920 (Garner and Allard, 1920). Photoperiod is indeed an essential cue that allows plants to distinguish between seasons and initiate flowering at the optimal time. Whether and when plants flower when grown under different photoperiods is a reliable indicator of their photoperiod sensitivity. In plants, photoperiod sensitivity directly shapes their latitudinal adaptation and yield (Lu et al., 2017). Because of its significant influence on plant development and agricultural

productivity, photoperiod sensitivity has garnered substantial attention from plant physiologists and breeders worldwide. Based on their responses to day length, plants can be classified into LD, SD plants, and day-neutral plants.

We previously focused on the role of the EC in the typical SD plant soybean, investigating the consequences of loss of EC components on flowering time and photoperiod sensitivity (Lu et al., 2017; Bu et al., 2021; Zhao et al., 2024). Specifically, the soybean homolog of GI, E2, forms a feedback loop with the EC, with E2 associating with FKF1 to degrade J (the soybean ELF3 homolog), while the EC also inhibits *E2* transcription. This antagonistic regulatory cycle between E2 and the EC determines soybean photoperiod sensitivity (Zhao et al., 2024). By contrast, GI does not reciprocally influence the protein levels of ELF3 in the facultative LD plant species Arabidopsis, suggesting some level of divergence in the regulatory mechanisms of this module between soybean and Arabidopsis. and sparking our interest in exploring how photoperiod sensitivity is regulated in Arabidopsis, an LD plant. The study of photoperiod sensitivity mechanisms, particularly those mediated by epigenetic regulation, remains relatively underexplored. Environmental responses via epigenetic regulation typically involve changes in histone modifications, DNA methylation, and RNA metabolism (Yaish et al., 2011; Nguyen et al., 2016). In this study, we proposed a model in which the LUX–SWI3C module regulates photoperiod sensitivity in Arabidopsis (Figure 5). Under SD conditions, more LUX binds at the *GI* transcription initiation site. The interaction between LUX and SWI3C strengthens, facilitating the recruitment of more SWI3C to the *GI* locus. This recruitment leads to greater chromatin compaction in the region, together with a corresponding decrease in H3K4me3 deposition, which suppresses *GI* transcription and results in delayed flowering. Conversely, under LD conditions, lower levels of LUX accumulate at the *GI* transcription start site. The interaction between LUX and SWI3C is weaker, leading to reduced recruitment of SWI3C to the *GI* locus. This results in a relatively loose chromatin structure and higher H3K4me3 deposition, which alleviates the inhibition of *GI* transcription and promotes early flowering. When either LUX or SWI3C is mutated, the other is unable to bind to the *GI* locus, resulting in nucleosome occupancy and H3K4me3 levels conducive to activating *GI* expression to the threshold required for flowering. Hence,

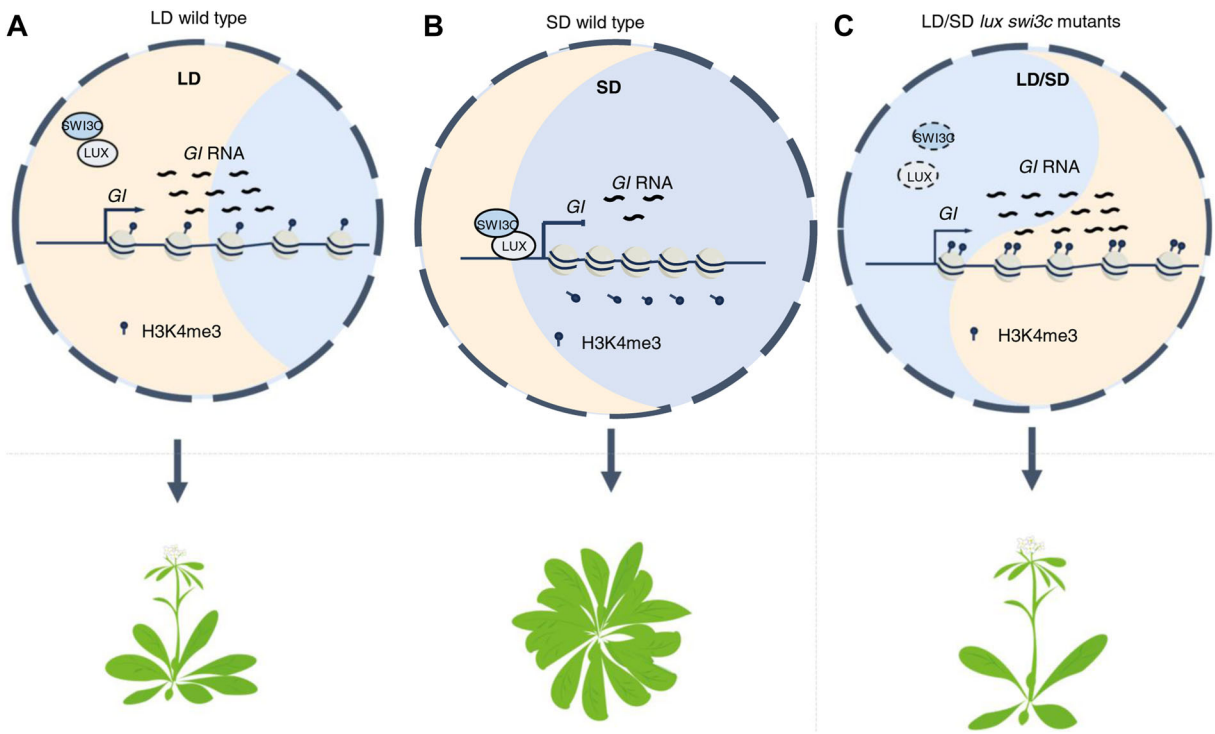

Figure 5. Proposed model for the LUX and SWI3C regulation of photoperiod sensitivity

(A) Under long-day (LD) conditions, LUX abundance is low, with little LUX binding near the *GI* transcription start site and LUX recruiting low levels of SWI3C to the *GI* locus. The chromatin at the *GI* locus thus takes on a relaxed structure, with increased levels of H3K4me3 modification, thus facilitating a transcriptionally active state around *GI* and leading to higher *GI* expression levels, promoting flowering in Arabidopsis. **(B)** By contrast, under short-day (SD) conditions, the quantity of LUX protein bound to the *GI* promoter is significantly enhanced and the interaction between LUX and SWI3C also strengthens, facilitating the recruitment of more SWI3C to this location and leading to greater chromatin compaction, together with a corresponding decrease in H3K4me3 accumulation, suppressing *GI* transcription and resulting in delayed flowering. **(C)** In the *lux swi3c* double mutants or their single mutants, LUX cannot recruit SWI3C to the *GI* locus, thus preventing the regulation of chromatin compaction at the *GI* locus under both LD and SD conditions. Consequently, the chromatin remains open with high H3K4me3 levels, rendering the *GI* locus transcriptionally active and resulting in a loss of photoperiod sensitivity.

the mutants lose photoperiod sensitivity. Therefore, we suggest that LUX and SWI3C participate in the regulation of photoperiod sensitivity in Arabidopsis.

To uncover the mechanisms of photoperiod sensitivity, it is crucial to identify mutants with altered photoperiod sensitivity, preferably those that have lost photoperiod sensitivity. Previous reports have indicated that the EC plays a central role in photoperiodic flowering in Arabidopsis, rice, maize, pea, and soybean. However, their target genes vary among species (Liew et al., 2009; Weller and Ortega, 2015; Li et al., 2016b; Lu et al., 2017; Andrade et al., 2022). Interestingly, in Arabidopsis, LUX can form a complex with HOS1 and HDA9 that regulates *GI* expression and mediates the photoperiodic pathway, but this model applies only under LD conditions (Park et al., 2019). In this study, we primarily focused on the mechanisms of photoperiod sensitivity. The *lux-6* mutant exhibited early flowering under both LD and SD conditions, consistent with previous findings (Hazen et al., 2005). Notably, the *lux-6* mutant flowered with the same number of rosette leaves when grown under LD and SD conditions. Thus, *LUX* plays a key role in photoperiod sensitivity and provides a valuable tool for dissecting this signaling pathway. Therefore, we looked for proteins that interacted with LUX to elucidate this mechanism.

We generated various double-mutant lines between *lux-6* and key genes involved in the photoperiodic pathway, which revealed that LUX acted upstream of *GI*; this parallels previous findings of the HOS15–EC–HDA9 module regulating *GI* expression (Park et al., 2019). Subsequent Y2H screening identified an interaction between LUX and SWI3C, which we validated by *in vivo* and *in vitro* experiments. Importantly, the *swi3c-3* mutant was also insensitive to photoperiod, suggesting SWI3C as a potential component that interacts with LUX to jointly regulate photoperiod sensitivity in Arabidopsis. Under these two extreme photoperiod conditions, the similar flowering times observed in both the *lux-6* and *swi3c-3* mutants underscores their complete loss of photoperiod sensitivity, suggesting that LUX and SWI3C are important components in the regulation of photoperiod sensitivity. Generally, upstream components transduce signals to their downstream targets. We wondered whether LUX and SWI3C might differ in their signal perception under different photoperiod conditions. Therefore, we compared the abundance and interaction strengths of the LUX–SWI3C interaction under different photoperiods (Figures 2D, S3A–E). LUX and SWI3C levels showed no significant differences between SD and LD conditions. Additionally, the interaction strength between LUX and SWI3C was stronger under SD conditions than under LD conditions.

As a critical subunit of the BRAHMA-related SWI/SNF complex (BAS), SWI3C functions in transcriptional regulation to modulate access to transcription factors to their respective *cis*-regulatory elements (Guo et al., 2022; Fu et al., 2023). Chromatin remodeling factors such as SWI3C slide, move, or replace nucleosomes at specific sites through ATP hydrolysis, exposing *cis*-elements and relaxing chromatin structure, and thus facilitating transcription (Clapier et al., 2017). Typically, chromatin remodeling is also associated with histone modification cross-talk. According to previous studies, SWI3C is associated with the H3K4me3, H3K27me3, and H3ac modifications (Li et al., 2016a; Guo et al., 2022; Yang et al., 2022). However, in our study, we found that the H3K27me3 signal at the *GI* locus was very weak, with detectable signals only at Sites 3 and 4, showing no differences among genotypes, and with no changes in H3ac levels; SWI3C appears to be involved only in the regulation of H3K4me3 deposition. This mechanism is similar to that seen with the BAS complex component BRM regulating H3K4me3 at the *SOC1* locus controlled by GATA, NITRATE-INDUCIBLE, CARBON METABOLISM INVOLVED (GNC), where H3K27me3 levels also remained unchanged (Yang et al., 2022). As SWI3C lacks H3K4me3 demethylase activity, identifying the specific histone H3K4me3 demethylase(s) involved in photoperiod sensitivity is a future research direction.

In this study, we showed that LUX and SWI3C interact and regulate downstream gene expression in an interdependent manner (Figure 2). The transcription factor LUX recognizes its cognate binding sites, while the chromatin remodeling factor SWI3C alters the epigenetic landscape at and near these sites, rendering both factors essential for the process. Previous studies suggested that LUX regulates downstream transcription mainly as a transcriptional repressor (Hazen et al., 2005). However, our findings indicate that the LUX role is limited to recognizing binding sites, and its transcriptional repression function is primarily executed by SWI3C. Under SD conditions, the strengthened LUX–SWI3C interaction led to greater LUX binding to the *GI* transcription start site, recruiting a large amount of SWI3C to this site, leading to chromatin compaction and diminished H3K4me3 accumulation, thereby repressing *GI* transcription and resulting in delayed flowering. Conversely, under LD conditions, the weakened LUX–SWI3C interaction results in only a small amount of LUX binding near the *GI* transcription start site, and thus recruited little SWI3C, leading to a relatively loose chromatin structure and increased H3K4me3 accumulation, therefore promoting *GI* transcription and resulting in earlier flowering. When *LUX* or *SWI3C* is mutated, *GI* transcription remains permanently activated, causing Arabidopsis plants to completely lose photoperiod sensitivity (Figure 5). Our model suggests that the LUX/SWI3C-*GI* epigenetic regulatory module contributes to photoperiod sensitivity in Arabidopsis, with our study focusing on the transcriptional regulation of *GI*. This may be only one of the roles played by this module, as this module may regulate additional target genes. For example, in rice, the EC regulates flowering under LD and SD conditions by modulating *OsPRR37* and *OsGhd7* expression levels (Andrade et al., 2022). Similarly, in Arabidopsis, EC target genes are not limited to *GI*. Key EC target genes within the circadian clock include *PRR9* and *PRR7* (Kolmos et al., 2011; Herrero et al., 2012). *PRR7* and *PRR9* along with *PRR5* are genetically redundant for the control of flowering time and

hypocotyl length (Nakamichi et al., 2005). Additionally, the *prr7 prr9* double mutant largely suppresses the early-flowering phenotype of *elf3* (Yuan et al., 2024), suggesting that part of the mechanism regulating photoperiodic sensitivity, besides the regulation of *GI* (and eventually *CO*) expression patterns, may involve the direct regulation of CO levels through control of *PRR* mRNA levels and, eventually, the levels of their encoded proteins. Other target genes may be involved in the LUX–SWI3C-mediated regulation of photoperiod sensitivity. Identifying additional target genes involved in LUX–SWI3C-mediated regulation of photoperiod sensitivity will be an important task. Interestingly, the transcriptional regulation of *GI* by LUX diverges between the SD plant soybean and the LD plant Arabidopsis. Unlike LUX in Arabidopsis, which regulates *GI* transcription under both LD and SD conditions, in soybean, LUX in soybean regulates *E2* (the *GI* homolog) expression only under LD conditions.

Unveiling the full spectrum of molecular mechanisms behind photoperiod sensitivity raises several intriguing questions. For instance, Arabidopsis continuously monitors changes in photoperiod through photoreceptors present in its leaves, and then transmits this signal to downstream response genes. A key question is why the enrichment levels of LUX/SWI3C at *GI* differ under various photoperiod conditions. This variability may arise from upstream proteins affecting the stability of LUX or SWI3C or their post-translational modifications. Notably, research in soybean has shown that the phytochromes phyA2 and phyA3 can degrade LUX by directly interacting with it as part of the EC, thus alleviating the repression of *E1* imposed by LUX, a critical step in photoperiodic flowering (Lin et al., 2022). Similarly, in rice, phyB affects the activity of ELF3, influencing photoperiod perception (Andrade et al., 2022). In Arabidopsis, mutation of *PHYB* leads to the loss of photoperiod sensitivity, and the *phyB-9* mutant showed additive effects with the loss of *LUX* and *SWI3C* (Figures 1, 2), suggesting a complex interaction that might influence the activity of the LUX/SWI3C-*GI* module under different photoperiods. Additionally, phyB might directly transmit photoperiod signals to the EC, suggesting that a similar mechanism might exist in Arabidopsis with phyB regulating EC or SWI3C activity. Addressing these critical questions is a direction for future research.

MATERIALS AND METHODS

Plant materials and growth conditions

The *Arabidopsis thaliana* accession Columbia (Col-0) was the genetic background for all plant lines used in this study, encompassing the wild-type, mutants, and transgenic lines. The seeds underwent stratification at 4°C in the dark for 3 d to promote uniform germination. Post-stratification, seeds were released in a greenhouse, and subjected to either an LD photoperiod (16-h light/8-h dark) or an SD photoperiod (8-h light/16-h dark). Four days post-emergence, seedlings were transplanted into soil. The growth environment was consistently maintained at 22°C.

The mutants used in this study included: *lux-6* (SALK132224), *swi3c-3* (SAIL_224_B10), *swi3c-2* (Koncz_3737), *gi-201* (SALK-092757), *co-10* (SAIL_24_H04), *soc1-2* (*agl20*), *elf3-1* (Zhang et al., 2018), *elf4-209* (N86619), *ft-10* (GK-290E08), and *phyb-9* (*hy3-EMS142*).

The *swi3c proSWI3C:SWI3C-GFP* transgenic plants were obtained by cloning a 1,799-bp *SWI3C* promoter fragment and the *SWI3C* cDNA was prepared from total RNA extracted from whole seedlings into the pCAMBIA1300 binary vector. The resulting construct was transformed into Agrobacterium (*Agrobacterium tumefaciens*) strain GV3101; positive colonies were cultured at 28°C for 3 d before transformation of *swi3c-3* mutant plants via the floral dip method (Clough and Bent, 1998). Transgenic plants were selected for resistance to hygromycin B; T3 homozygous transgenic lines were used for analysis.

Yeast-two-hybrid assays

Yeast two-hybrid assays were conducted following the guidelines provided in the manual for the GAL4-based Matchmaker Two-Hybrid System 3 (Clontech). The full-length coding sequences of *LUX* and *SWI3C* were subcloned into thepGADT7 and pGBKT7 vectors, respectively. The primers employed for these constructs are listed in Table S2. Subsequently, Pairs of AD and BD constructs were co-transformed into the yeast strain AH109 via the lithium acetate method as described in the Yeast Protocols Handbook (Clontech). The transformed yeast cells were initially plated on a synthetic defined medium lacking leucine and tryptophan (SD/−Leu/−Trp) to select positive co-transformants. These co-transformants were then assessed for protein–protein interaction potential by transferring them onto SD medium lacking leucine, tryptophan, adenine, and histidine (SD/−Leu/−Trp/−Ade/−His).

Yeast-three-hybrid assays

The full-length *LUX* coding sequence was cloned into the MCS1 of the pBridge vector, while the full-length coding sequence of *ELF3* or *ELF4* was inserted into the MCS2 of the pBridge vector. The indicated pairs of AD and pBridge constructs were co-transferred into yeast strain AH109, and the yeast transformants were spread onto SD/−Leu/−Trp plates for positive colony selection at 30°C for 48–60 h. Then, the transformants were cultured in liquid SD/−Leu/−Trp medium at 30°C with shaking at 200 rpm overnight. After transfer to liquid SD/−Leu/−Trp/−Met medium for 3 h, 1 mL of yeast culture was harvested by centrifugation for 5 min at 10,000 *g* and washed once in Z buffer (pH 7.0) consisting of 21.5 g/L $Na_2HPO_4{\cdot}12H_2O$, 6.2 g/L $NaH_2PO_4{\cdot}2H_2O$, 0.75 g/L KCl, 0.246 g/L $MgSO_4{\cdot}7H_2O$. After centrifugation, the cell pellets were resuspended in 150 μL of *Z* buffer containing 0.27% (v/v) β-mercaptoethanol, 50 μL chloroform, and 20 μL 0.1% (w/v) sodium dodecyl sulfate (SDS), and vortexed vigorously for 15 s. The reactions were incubated at 37°C after adding

200 μL of 4 g/L *o*-nitrophenol-β-D-galactopyranoside (ONPG; dissolved in *Z* buffer), and the time of ONPG addition was recorded. When a reaction turned yellow, 500 μL of 1 M Na_2CO_3 was added to stop the reaction and the time was recorded. The mixtures were then centrifuged, the supernatants were collected, and their absorbance at 420 nm (A420) was measured, using absorbance at 600 nm (A600) to estimate yeast cell count. The β-galactosidase units were calculated as below.

$$\text{Miller Units} = 1000 * A420/[A600 * \text{culture volume (mL)} * \text{reaction time (min)}]$$

Luciferase complementation imaging assays

The full-length *LUX* coding sequence was cloned into the pCAMBIA1300-NLUC vector, while the full-length *SWI3C* coding sequence was inserted into the pCAMBIA1300-CLUC vector. The resulting constructs were individually transformed into Agrobacterium strain GV3101. Appropriate pairs of positive Agrobacterium cultures were then co-infiltrated into the leaves of *Nicotiana benthamiana* plants. The volume of Agrobacterium required for the combination was calculated by measuring the optical density at 600 nm using a spectrophotometer, and the calculation formulas are as follows:

$$V_{sample} = V_{final} \times 0.5/OD600 \times n$$

$$V_{P19} = V_{final} \times 0.3/OD600 \times n$$

The volume of bacterial liquid required for different samples and P19 in each combination according to the above formulas were calculated. The silencing suppressor P19 should be added to each reaction combination, and mixed in a centrifuge tube. The mixture was centrifuged at 12,000 *g* for 2 min at room temperature to collect the bacteria. The bacteria were suspended with 2 mL of resuspension solution (10 mM MES-KOH (pH 5.7), 40 mM $MgCl_2$, 0.15 mM acetosyringone), and placed at room temperature for 2–5 h before injecting into tobacco leaves. After a period of 48 h post-infiltration to allow for expression, firefly luciferase (LUC) activity was detected using a cold charge-coupled device (CCD) camera. The D-Luciferin sodium salt (16291; kingbio) was sprayed onto the leaves. The concentration of the solution used was 8.79 mM (diluted 100 times for use), and a waiting time of 5 min was observed before taking photographs.

Bimolecular fluorescence complementation assays

To prepare vectors for the BiFC assay, the full-length *SWI3C* coding sequence was cloned into the pUC–SPYCE vector, while the full-length *LUX* coding sequence was cloned into the pUC–SPYNE vector. The resulting constructs were individually transformed into Agrobacterium strain GV3101. Appropriate pairs of positive Agrobacterium cultures were then co-infiltrated into the leaves of *N. benthamiana* plants. Infiltrated plants were maintained under a 16-h light/8-h dark photoperiod for about 2 d. Yellow fluorescent protein (YFP) fluorescence was observed under a confocal laser-scanning microscope (Zeiss).

GST pull-down assay

The GST pull-down assay was conducted as previously described with some modifications (Yang et al., 2022). The full-length *LUX* coding sequence was cloned into the pGEX4T-1 vector; similarly, the full-length *SWI3C* coding sequence was cloned into the pET28(a) vector. These constructs were introduced into *Escherichia coli* BL21 cells and positive colonies were cultured at 20°C for 10 h, using 0.3 mM isopropylthio-β-galactoside (IPTG) to induce protein production. For the binding assay, recombinant purified 10 μg GST or GST-LUX was combined with GST resin (GE Healthcare, USA) and incubated in buffer (50 mM Tris-HCl, pH 7.4; 5% (v/v) glycerol; 120 mM NaCl; 0.5% (v/v) Nonidet P-40; 1 mM β-mercaptoethanol; and 1 mM phenylmethylsulfonyl fluoride (PMSF)) for 2 h at 4°C. Post incubation, these complexes were mixed with a supernatant containing His-tagged SWI3C and incubated at 25°C for 60 min. Following five washes with wash buffer (50 mM Tris-HCl, pH 7.4; 5% (v/v) glycerol; 120 mM NaCl; and 0.5% (v/v) Nonidet P-40), the bound proteins were eluted by boiling in SDS sample buffer. The protein–protein interactions were analyzed through SDS-PAGE gel electrophoresis followed by immunoblotting. For immunoblotting, anti-GST (HT601-01; with a working dilution at a ratio of 1:5,000; TransGen) and anti-HIS (HT501-01; with a working dilution at a ratio of 1:1,000; TransGen) antibodies were used.

Co-immunoprecipitation assay assays

The co-IP assay was performed as previously described with some modifications (Gu et al., 2017). Protein was extracted from 14-d-old seedlings grown on Murashige and Skoog (MS) medium under SD or LD conditions, using a buffer containing 50 mM Tris-HCl (pH 7.4), 2 mM $MgCl_2$, 150 mM NaCl, 1 mM DTT, 1% (v/v) NP-40, 20% (v/v) glycerol, 0.05 mM MG132, and 2 mM PMSF, supplemented with a protease inhibitor cocktail from Roche. The resulting supernatant was then incubated with 30 μL of GFP-Trap®-A beads (Chromo Tek) at 4°C for 4 h. Following incubation, the beads were centrifuged for collection (at 4°C, 1,000 *g*) and washed six times in buffer (2 mM $MgCl_2$; 50 mM Tris-HCl, pH 7.4; 150 mM NaCl; 1% (v/v) NP-40; 1 mM DTT; and 10% (v/v) glycerol). The proteins bound to the beads were eluted with 40 μL of 2× SDS loading buffer and subsequently analyzed via immunoblotting. For immunoblotting, anti-GFP (HT801-01; with a working dilution at a ratio of 1:5,000; TransGen) and anti-LUX (R1247-4; with a working dilution at a ratio of 1:1,000; Abiocode) antibodies were used.

Protein extraction method

Total protein was extracted as described previously (Qiu et al., 2017; Han et al., 2023). Briefly, Arabidopsis seedlings

were ground and homogenized in extraction buffer (100 mM Tris-HCl, pH 7.5; 100 mM NaCl; 5 mM EDTA, pH 8.0; 20% (w/v) glycerol; 5% (w/v) SDS; 40 mM β-mercaptoethanol; 20 mM DTT; 2 mM PMSF; 80 μM MG132; 80 μM MG115; 1× EDTA-free protease inhibitor cocktail; and 1% (v/v) phosphatase inhibitor cocktail). Samples were boiled for 10 min, followed by centrifugation at 16,000 *g* for 15 min at room temperature. The supernatants were collected and used for immunoblotting. To detect the protein levels of LUX and SWI3C, the band intensity of the target protein was normalized to that of actin (or a non-specific band). Specifically, the band gray values of the target protein and actin protein (or non-specific band) were measured separately using ImageJ image analysis software. The gray value reflects the signal intensity of the protein band. Then, the gray value of the target protein was divided by that of actin (or the non-specific band) to obtain the expression ratio of the target protein relative to actin (or the non-specific band). The ratio obtained through the above-mentioned normalization process is the relative expression level of the target protein. This relative expression level can be used to compare the expression differences of the target protein among different samples.

Reverse transcription qPCR analysis

Total RNA was isolated from 14-d-old seedlings grown on MS medium, using TRIzol™ reagent (Cat. No. 644 15596026; Invitrogen). Total RNA was then converted to first-strand cDNA, employing approximately 1 μg of total RNA with a SuperScript First-strand cDNA Synthesis System (TaKaRa), following the guidelines provided by the manufacturer. The resulting cDNA served as a template for qPCR analysis, which was performed using a PrimeScript RT reagent kit (TaKaRa). In this analysis, *UBQ10* was selected as the reference gene. Three biological replicates were conducted in each experiment. The specific primers used for the RT-qPCR are listed in Table S2.

Chromatin immunoprecipitation assays

The ChIP assays were conducted based on a previously established protocol (Gendrel et al., 2005). Chromatin was extracted from 14-d-old seedlings after fixation with 1% (w/v) formaldehyde, followed by vacuum incubation for 15 min. The extracted chromatin was then fragmented to an average size of about 600 bp through sonication. The samples were sonicated in an ice–water mixture at 30% power, with a cycle of 1 s on and 9 s off, for a total of 90 cycles. Following fragmentation, specific antibodies were used for immunoprecipitation: anti-H3K4me3 (ab8580; Abcam), anti-H3K27me3 (07-449; Millipore), anti-H3ac (ab47915; Abcam), and anti-GFP (ab290; Abcam). After immunoprecipitation, the DNA–protein cross-links were reversed following the method described previously (Gendrel et al., 2005). The quantity of specific targets immunoprecipitated was then determined via qPCR, using the gene-specific primers listed in Table S2.

MNase-qPCR assays

Next, 14-d-old seedlings (0.3 g fresh weight per sample) were cross-linked with 1% (w/v) formaldehyde and then frozen in liquid nitrogen. Nuclei and chromatin were isolated according to the method by Han et al. (2012). The chromatin was then digested with micrococcal nuclease (TaKaRa) at a final concentration of 0.2 units/mL for 10 min at 37°C in the supplied digestion. Subsequent procedures were carried out as detailed by Chodavarapu et al. (2010). Mononucleosomes were extracted from 1.5% (w/v) agarose gels and purified using a Qiagen gel purification kit (28506). The input fraction was determined as $2^{-\Delta\Delta Ct}$ ($2^{-[Ct(mono) - Ct(gDNA)]}$) using undigested genomic DNA (Gévry et al., 2009). The specific primers used for the assay are listed in Table S2.

In vitro cell-free *in vitro* degradation assays

For cell-free degradation assays, total proteins were extracted from Col-0, *lux-6*, *swi3c-3*, and *lux-6 swi3c-3* 14-d-old seedlings grown under different photoperiod conditions (SD or LD) with cell-free extraction buffer (50 mM Tris-MES, pH 8.0; 0.5 M sucrose; 1 mM $MgCl_2$; 10 mM EDTA, pH 8.0; and 5 mM DTT). To 200 μg of each whole-protein extract, 0.1 μg purified recombinant GI was added together with 10 mM ATP and incubated at 25°C. Aliquots were taken at the indicated times and proteins were separated by SDS-PAGE and detected with an anti-MBP antibody (HT701; with a working dilution at a ratio of 1:5,000; TransGen Biotech). Actin was used as a loading control (CW0096M; the working dilution at a ratio of 1:5,000; CWBIO).

ACKNOWLEDGEMENTS

We extend our gratitude to Dr. Songguang Yang from the Guangdong Academy of Agricultural Sciences for generously providing the *swi3c-2*, *swi3c-3*, and *proSWI3C:SWI3C-GFP* seeds. We also thank Professor Lei Wang from the Chinese Academy of Sciences, Professor Qiguang Xie from Henan University and Professor Wei Huang from South China Agricultural University for providing Arabidopsis mutant seeds. The research was supported by the Joint Funding Project of Guangzhou Municipal Government, Universities (Academies) and Enterprises (2023A03J0049 to F.K.), the Open Competition Program of Top Ten Critical Priorities of Agricultural Science and Technology Innovation for the 14th Five-Year Plan of Guangdong Province (2022SDZG05 to F.K. and B.L.), and the National Natural Science Foundation of China (32090064 to F.K., 32301824 to J.W., 32401857 to Z.S., 32201866 to F.W., and 32301823 to Hu. L.).

CONFLICTS OF INTEREST

The authors declare no competing interests.

AUTHOR CONTRIBUTIONS

F.K. and J.W. designed the research; J.W. and Z.S. performed most of the research. J.W. and Z.S. drafted the manuscript. Hu. L. conducted yeast-three-hybrid experiment, Ho. L. detected the changes in protein levels of LUX and SWI3C under LD and SD conditions. F.W., S.Y., L.Y., S.L., B.L., and M.H. conducted supervised research and revised the manuscript.

Edited by: Xiaodong Xu, Henan University, China

Received Oct. 30, 2024; **Accepted** Feb. 18, 2025

REFERENCES

An, H., Roussot, C., Suárez-López, P., Corbesier, L., Vincent, C., Piñeiro, M., Hepworth, S., Mouradov, A., Justin, S., Turnbull, C. et al. (2004). CONSTANS acts in the phloem to regulate a systemic signal that induces photoperiodic flowering of Arabidopsis. Development **131:** 3615–3626.

Andrade, L., Lu, Y., Cordeiro, A., Costa, J.M.F., Wigge, P.A., Saibo, N.J.M., and Jaeger, K.E. (2022). The evening complex integrates photoperiod signals to control flowering in rice. Proc. Natl. Acad. Sci. U.S.A. **119:** e2122582119.

Archacki, R., Sarnowski, T.J., Halibart-Puzio, J., Brzeska, K., Buszewicz, D., Prymakowska-Bosak, M., Koncz, C., and Jerzmanowski, A. (2009). Genetic analysis of functional redundancy of BRM ATPase and ATSWI3C subunits of Arabidopsis SWI/SNF chromatin remodelling complexes. Planta **229:** 1281–1292.

Bu, T., Lu, S., Wang, K., Dong, L., Li, S., Xie, Q., Xu, X., Cheng, Q., Chen, L., Fang, C., et al. (2021). A critical role of the soybean evening complex in the control of photoperiod sensitivity and adaptation. Proc. Natl. Acad. Sci. U.S.A. **118:** e2010241118.

Chodavarapu, R.K., Feng, S., Bernatavichute, Y.V., Chen, P.Y., Stroud, H., Yu, Y., Hetzel, J.A., Kuo, F., Kim, J., Cokus, S.J., et al. (2010). Relationship between nucleosome positioning and DNA methylation. Nature **7304:** 388–392.

Clapier, C.R., Iwasa, J., Cairns, B.R., and Peterson, C.L. (2017). Mechanisms of action and regulation of ATP-dependent chromatin-remodelling complexes. Nat. Rev. Mol. Cell Biol. **18:** 407–422.

Clough, S.J., and Bent, A.F. (1998). Floral dip: A simplified method for Agrobacterium mediated transformation of *Arabidopsis thaliana*. Plant J. **16:** 735–743.

Corbesier, L., Vincent, C., Jang, S., Fornara, F., Fan, Q., Searle, I., Giakountis, A., Farrona, S., Gissot, L., Turnbull, C., et al. (2007). FT protein movement contributes to long-distance signaling in floral induction of Arabidopsis. Science **316:** 1030–1033.

Creux, N., and Harmer, S. (2019). Circadian rhythms in plants. Cold Spring Harb. Perspect. Biol. **11:** a034611.

Doyle, M.R., Davis, S.J., Bastow, R.M., McWatters, H.G., Kozma-Bognár, L., Nagy, F., Millar, A.J., and Amasino, R.M. (2002). The ELF4 gene controls circadian rhythms and flowering time in *Arabidopsis thaliana*. Nature **419:** 74–77.

Ezer, D., Jung, J.-H., Lan, H., Biswas, S., Gregoire, L., Box, M.S., Charoensawan, V., Cortijo, S., Lai, X., Stöckle, D., et al. (2017). The evening complex coordinates environmental and endogenous signals in *Arabidopsis*. Nat. Plants. **3:** 17087.

Fornara, F., Panigrahi, K.C.S., Gissot, L., Sauerbrunn, N., Rühl, M., Jarillo, J.A., and Coupland, G. (2009). Arabidopsis DOF transcription factors act redundantly to reduce *CONSTANS* expression and are essential for a photoperiodic flowering response. Dev. Cell **17:** 75–86.

Fu, W., Yu, Y., Shu, J., Yu, Z., Zhong, Y., Zhu, T., Zhang, Z., Liang, Z., Cui, Y., Chen, C., et al. (2023). Organization, genomic targeting, and assembly of three distinct SWI/SNF chromatin remodeling complexes in *Arabidopsis*. Plant Cell **35:** 2464–2483.

Garner, W.W., and Allard, H.A. (1920). Effect of the relative length of day and night and other factors of the environment on growth and reproduction in plants. J. Agric. Res. **18:** 553–606.

Gendrel, A.V., Lippman, Z., Martienssen, R. andColot, V. (2005). Profiling histone modification patterns in plants using genomic tiling microarrays. Nat. Methods **2:** 213–218.

Gévry, N., Svotelis, A., Larochelle, M., and Gaudreau, L. (2009). Nucleosome mapping. Methods Mol. Biol. **543:** 281–291.

Gu, D., Chen, C.-Y., Zhao, M., Zhao, L., Duan, X., Duan, J., Wu, K., and Liu, X. (2017). Identification of HDA15-PIF1 as a key repression module directing the transcriptional network of seed germination in the dark. Nucleic Acids Res. **45:** 7137–7150.

Guo, J., Cai, G., Li, Y.Q., Zhang, Y.X., Su, Y.N., Yuan, D.Y., Zhang, Z.C., Liu, Z.Z., Cai, X.W., Guo, J., et al. (2022). Comprehensive characterization of three classes of *Arabidopsis* SWI/SNF chromatin remodelling complexes. Nat. Plants. **8:** 1423–1439.

Han, R., Ma, L., Lv, Y., Qi, L., Peng, J., Li, H., Zhou, Y., Song, P., Duan, J., Li, J., et al. (2023). SALT OVERLY SENSITIVE2 stabilizes phytochrome-interacting factors PIF4 and PIF5 to promote Arabidopsis shade avoidance. Plant Cell **35:** 2972–2996.

Han, S.K., Sang, Y., Rodrigues, A., BIOL425, F.2010, Wu, M.F., Rodriguez, P.L., and Wagner, D. (2012). The SWI2/SNF2 chromatin remodeling ATPase BRAHMA represses abscisic acid responses in the absence of the stress stimulus in *Arabidopsis*. Plant Cell **12:** 4892–4906.

Hazen, S., Schultz, T., Pruneda-Paz, J., Borevitz, J., Ecker, J., and Kay, S. (2005). LUX ARRHYTHMO encodes a Myb domain protein essential for circadian rhythms. Proc. Natl. Acad. Sci. U.S.A. **102:** 10387–10392.

Herrero, E., and Davis, S.J. (2012). Time for a nuclear meeting: Protein trafficking and chromatin dynamics intersect in the plant circadian system. Mol. Plant **5:** 554–565.

Herrero, E., Kolmos, E., Bujdoso, N., Yuan, Y., Wang, M., Berns, M.C., Uhlworm, H., Coupland, G., Saini, R., Jaskolski, M., et al. (2012). EARLY FLOWERING4 recruitment of EARLY FLOWERING3 in the nucleus sustains the Arabidopsis circadian clock. Plant Cell **24:** 428–443.

Huang, H., Alvarez, S., Bindbeutel, R., Shen, Z., Naldrett, M.J., Evans, B.S., Briggs, S.P., Hicks, L.M., Kay, S.A., and Nusinow, D.A. (2016). Identification of evening complex associated proteins in Arabidopsis by affinity purification and mass spectrometry. Mo. Cell. Proteomics **15:** 201–217.

Imaizumi, T., Schultz, T.F., Harmon, F.G., Ho, L.A., and Kay, S.A. (2005). FKF1 F-Box protein mediates cyclic degradation of a repressor of CONSTANS in Arabidopsis. Science **309:** 293–297.

Jung, J.H., Barbosa, A.D., Hutin, S., Kumita, J.R., Gao, M., Derwort, D., Silva, C.S., Lai, X., Pierre, E., Geng, F., et al. (2020). A prion-like domain in ELF3 functions as a thermosensor in Arabidopsis. Nature **585:** 256–260.

Kikis, E.A., Khanna, R., and Quail, P.H. (2005). ELF4 is a phytochrome—regulated component of a negative—feedback loop involving the central oscillator components CCA1 and LHY. Plant J. **44:** 300–313.

Kolmos, E., Herrero, E., Bujdoso, N., Millar, A.J., Tóth, R., Gyula, P., Nagy, F., and Davis, S.J. (2011). A reduced-function allele reveals that EARLY FLOWERING3 repressive action on the circadian clock is modulated by phytochrome signals in Arabidopsis. Plant Cell **23:** 3230–3246.

Kwon, Y., Kim, C., and Choi, G. (2024). Phytochrome B photobody components. New Phytol. **242:** 909–915.

Li, C., Gu, L., Gao, L., Chen, C., Wei, C.Q., Qiu, Q., Chien, C.W., Wang, S., Jiang, L., Ai, L.F., et al. (2016a). Concerted genomic targeting of H3K27 demethylase REF6 and chromatin-remodeling ATPase BRM in *Arabidopsis*. Nat. Genet. **48:** 687–693.

Li, J., Hu, E., Chen, X., Xu, J., Lan, H., Li, C., Hu, Y., and Lu, Y. (2016b). Evolution of DUF1313 family members across plant species and their association with maize photoperiod sensitivity. Genomics **107:** 199–207.

Liew, L.C., Hecht, V., Laurie, R.E., Knowles, C.L., Vander Schoor, J.K., Macknight, R.C., and Weller, J.L. (2009). DIE NEUTRALIS and LATE BLOOMER 1 contribute to regulation of the pea circadian clock. Plant Cell **21:** 3198–3211.

Lin, X., Dong, L., Tang, Y., Li, H., Cheng, Q., Li, H., Zhang, T., Ma, L., Xiang, H., Chen, L., et al. (2022). Novel and multifaceted regulations of photoperiodic flowering by phytochrome A in soybean. Proc. Natl. Acad. Sci. U.S.A. **119:** e2208708119.

Liu, S., He, M., Lin, X.and Kong, F. (2023). Epigenetic regulation of photoperiodic flowering in plants. Plant Genome **3:** e20320.

Liu, X.L., Covington, M.F., Fankhauser, C., Chory, J., and Wagner, D.R. (2001). *ELF3* encodes a circadian clock-regulated nuclear protein that functions in an Arabidopsis PHYB signal transduction pathway. Plant Cell **6:** 1293–1304.

Lu, S., Zhao, X., Hu, Y., Liu, S., Nan, H., Li, X., Fang, C., Cao, D., Shi, X., Kong, L., et al. (2017). Natural variation at the soybean J locus improves adaptation to the tropics and enhances yield. Nat. Genet. **49:** 773–779.

Nakamichi, N., Kita, M., Ito, S., Yamashino, T., and Mizuno, T. (2005). PSEUDO-RESPONSE REGULATORS, PRR9, PRR7 and PRR5, together play essential roles close to the circadian clock of *Arabidopsis thaliana*. Plant Cell Physiol. **46:** 686–698.

Nguyen, N.H., Jeong, C.Y., Lee, W.J., and Lee, H. (2016). Identification of a novel Arabidopsis mutant showing sensitivity to histone deacetylase inhibitors. Appl. Biol. Chem. **59:** 855–860.

Nusinow, D.A., Helfer, A., Hamilton, E.E., King, J.J., Imaizumi, T., Schultz, T.F., Farré, E.M., and Kay, S.A. (2011). The ELF4-ELF3-LUX complex links the circadian clock to diurnal control of hypocotyl growth. Nature **475:** 398–402.

Park, H.J., Baek, D., Cha, J.Y., Liao, X., Kang, S.H., McClung, C.R., Lee, S.Y., Yun, D.J., and Kim, W.Y. (2019). HOS15 interacts with the histone deacetylase HDA9 and the evening complex to epigenetically regulate the floral activator *GIGANTEA*. Plant Cell **31:** 37–51.

Qiu, Y., Pasoreck, E.K., Reddy, A.K., Nagatani, A., Ma, W., Chory, J., and Chen, M. (2017). Mechanism of early light signaling by the carboxy-terminal output module of Arabidopsis phytochrome B. Nat. Commun. **8:** 1905.

Samach, A., Onouchi, H., Gold, S.E., Ditta, G.S., Schwarz-Sommer, Z., Yanofsky, M.F., and Coupland, G. (2000). Distinct roles of CONSTANS target genes in reproductive development of Arabidopsis. Science **288:** 1613–1616.

Sarnowska, E.A., Rolicka, A.T., Bucior, E., Cwiek, P., Tohge, T., Fernie, A.R., Jikumaru, Y., Kamiya, Y., Franzen, R., Schmelzer, E., et al. (2013). DELLA-interacting SWI3C core subunit of switch/sucrose nonfermenting chromatin remodeling complex modulates gibberellin responses and hormonal cross talk in *Arabidopsis*. Plant Physiol. **163:** 305–317.

Sarnowski, T.J., Ríos, G., Jásik, J., Świeżewski, S., Kaczanowski, S., Li, Y., Kwiatkowska, A., Pawlikowska, K., Kozbiał, M., Kozbiał, P., et al. (2005). SWI3 subunits of putative SWI/SNF chromatin-remodeling complexes play distinct roles during Arabidopsis development. Plant Cell **17:** 2454–2472.

Sawa, M., Nusinow, D.A., Kay, S.A., and Imaizumi, T. (2007). FKF1 and GIGANTEA complex formation is required for day-length measurement in Arabidopsis. Science **318:** 261–265.

Shim, J.S., Kubota, A., and Imaizumi, T. (2017). Circadian clock and photoperiodic flowering in *Arabidopsis*: CONSTANS is a hub for signal integration. Plant Physiol. **173:** 5–15.

Silva, C.S., Lai, X., Nanao, M., and Zubieta, C. (2016). The Myb domain of LUX ARRHYTHMO in complex with DNA: Expression, purification and crystallization. Acta Crystallogr. F Struct. Biol. Commun. **72:** 356–361.

Song, Y.H., Shim, J.S., Kinmonth-Schultz, H.A., and Imaizumi, T. (2015). Photoperiodic flowering: Time measurement mechanisms in leaves. Annu. Rev. Plant Biol. **66:** 441–464.

Takagi, H., Hempton, A.K., and Imaizumi, T. (2023). Photoperiodic flowering in *Arabidopsis*: Multilayered regulatory mechanisms of CONSTANS and the florigen FLOWERING LOCUS T. Plant Commun. **4:** 100552.

Weller, J.L., and Ortega, R. (2015). Genetic control of flowering time in legumes. Front. Plant Sci. **6:** 207.

Wigge, P.A., Kim, M.C., Jaeger, K.E., Busch, W., Schmid, M., Lohmann, J.U., and Weigel, D. (2005). Integration of spatial and temporal information during floral induction in Arabidopsis. Science **309:** 1056–1059.

Yaish, M.W., Colasanti, J., and Rothstein, S.J. (2011). The role of epigenetic processes in controlling flowering time in plants exposed to stress. J. Exp. Bot. **62:** 3727–3735.

Yang, J., Xu, Y., Wang, J., Gao, S., Huang, Y., Hung, F.Y., Li, T., Li, Q., Yue, L., Wu, K., et al. (2022). The chromatin remodelling ATPase BRAHMA interacts with GATA-family transcription factor GNC to regulate flowering time in *Arabidopsis*. J. Exp. Bot. **73:** 835–847.

Yu, J.W., Rubio, V., Lee, N.Y., Bai, S., Lee, S.Y., Kim, S.S., Liu, L., Zhang, Y., Irigoyen, M.L., Sullivan, J.A., et al. (2008). COP1 and ELF3 control circadian function and photoperiodic flowering by regulating GI stability. Mol. Cell **32:** 617–630.

Yuan, L., Avello, P., Zhu, Z., Lock, S.C.L., McCarthy, K., Redmond, E.J., Davis, A.M., Song, Y., Ezer, D., Pitchford, J.W., et al. (2024). Complex epistatic interactions between ELF3, PRR9, and PRR7 regulate the circadian clock and plant physiology. Genetics **226:** iyad217.

Zhang, Y., Wang, Y., Wei, H., Li, N., Tian, W., Chong, K., and Wang, L. (2018). Circadian evening complex represses jasmonate-induced leaf senescence in Arabidopsis. Mol. Plant **11:** 326–337.

Zhao, L., Zhou, Q., He, L., Deng, L., Lozano Duran, R., Li, G., and Zhu, J.K. (2022). DNA methylation underpins the epigenomic landscape regulating genome transcription in Arabidopsis. Genome Biol. **23:** 197.

Zhao, X., Li, H., Wang, L., Wang, J., Huang, Z., Du, H., Li, Y., Yang, J., He, M., Cheng, Q., et al. (2024). A critical suppression feedback loop determines soybean photoperiod sensitivity. Dev. Cell **24:** 00229–6.

SUPPORTING INFORMATION

Additional Supporting Information may be found online in the supporting information tab for this article: http://onlinelibrary.wiley.com/doi/10.1111/jipb.13889/suppinfo

Figure 1. ELF3 and ELF4 do not affect the interaction between SWI3C and LUX

Figure 2. The *pSWI3C*:SWI3C-GFP/*swi3c-3* line has a normal photoperiod sensitivity, indicating that SWI3C-GFP is functional

Figure 3. Analysis of LUX and SWI3C protein levels under different conditions

Figure 4. Analysis of *CO, SOC1*, and *FT* gene expression levels

Figure 5. Analysis of LUX and SWI3C target genes and their associated histone modifications via chromatin immunoprecipitation sequencing (ChIP-seq)

Figure 6. Analysis of *in vivo* H3ac deposition at the *GI* locus

Figure 7. GI protein abundance in a cell-free degradation assay

Table S1. List of target genes shared by LUX and SWI3C
Table S2. List of primer sequences (5′–3′) used in this study
Table S3. Summary of statistical analyses for Figures 3A–B, 4A–B, S3F, S4 in this study

Scan the QR code to view JIPB on WeChat
(WeChat: **jipb1952**)

Scan the QR code to view JIPB on Twitter
(Twitter: **@JIPBio**)